Stellar Populations of Bulges in Galaxies with Low Surface-brightness Discs

Lorenzo Morelli[1,2]
Enrico Maria Corsini[1,2]
Alessandro Pizzella[1,2]
Elena Dalla Bontà[1,2]
Lodovico Coccato[3]
Jairo Méndez-Abreu[4,5]
Mary Cesetti[1,2]

[1] Dipartimento di Fisica e Astronomia, Università di Padova, Italy
[2] INAF–Osservatorio Astronomico di Padova, Italy
[3] ESO
[4] Instituto Astrofísico de Canarias, La Laguna, Spain
[5] Departamento de Astrofísica, Universidad de La Laguna, Spain

The radial profiles of the age, metallicity and α/Fe enhancement of the stellar populations in the bulge-dominated region for a sample of eight spiral galaxies with low surface-brightness stellar discs and bulges are presented. Almost all the sample bulges are characterised by young stellar populations, solar α/Fe enhancements and metallicities spanning from high to sub-solar values. No significant gradient in age and α/Fe enhancement is measured, whereas a negative metallicity gradient is found in a few cases. The stellar populations of the bulges hosted by low surface-brightness discs share many properties with those of high surface-brightness galaxies and are therefore likely to have common formation scenarios and evolution histories.

Galaxies with a central face-on surface brightness fainter than 22.6 mag per square arcsecond in the *B*-band are classified as low surface-brightness (LSB) systems. Although LSB galaxies are more difficult to identify than high-surface brightness (HSB) galaxies, they are not a niche phenomenon in galactic astrophysics. They constitute up to 50 % of the disc galaxy population and, consequently, they represent one of the major baryonic repositories in the Universe. LSB galaxies are characterised by different morphologies (ranging from dwarf irregulars to giant spirals) and they cover a wide range of colours which suggests that they can follow a variety of evolutionary paths (Bothun et al., 1997).

The typical gas surface density of LSB discs is below the critical threshold necessary for star formation, despite the fact that they have a higher content of neutral hydrogen than their HSB counterparts (Galaz et al., 2006). This inability to condense atomic gas into molecular gas results in a very low star formation rate and in a significantly slower evolution of the galaxy. Although most LSB galaxies are bulgeless, there are also galaxies with an LSB disc and a significant bulge component. It is not known whether these bulges are similar to those of HSB galaxies and whether their properties depend on the LSB nature of their host discs.

Invaluable pieces of information that help us to understand the processes of formation and evolution of bulges in LSB galaxies are imprinted in their stellar populations. The central values and radial profiles of age, metallicity and α/Fe enhancement of the stellar component can be used to test the predictions of theoretical models, as has already been done for the bulges of HSB galaxies (Sánchez-Blázquez et al., 2006; Annibali et al., 2007).

Gas dissipation toward the galaxy centre, with subsequent star formation and galactic winds, produces a gradient in the radial profile of metallicity. Therefore, a metallicity gradient is expected in bulges formed by monolithic collapse (Kobayashi, 2004), while the metallicity gradient is expected to be very shallow (or even absent) in bulges built by merging (Bekki & Shioya, 1999). Mergers of gas-poor galaxies mix up the galactic stars, erasing the pre-existing population gradients, and only rarely is the metallicity gradient enhanced by the secondary events of star formation, which eventually occur in mergers of gas-rich objects. If this latter occurs, a clear signature can be observed in the age radial profile for several Gyr (Hopkins et al., 2009). The predictions for bulges assembled through long timescale processes, such as the dissipationless secular evolution of the disc component, are more controversial. According to this scenario, the bulge is formed by the redistribution of disc stars and the gradients that are eventually produced in the progenitor disc could either be amplified, because the resulting bulge has a smaller scalelength than the disc, or could be erased as a consequence of disc heating (Moorthy & Holtzman, 2006).

We present a detailed photometric and spectroscopic study of a sample of eight bulges in LSB discs recently published by Morelli et al. (2012). The analysis of the spectral absorption lines has allowed us to derive the age and metallicity of the stellar populations and to estimate the efficiency and timescale of the last episode of star formation in order to distinguish between the early rapid assembly and late slow growth of the bulge.

Sample selection, surface photometry and long-slit spectroscopy

All the galaxies in this study were selected to be spiral galaxies with a bulge and an LSB disc. The final sample is comprised of eight LSB spiral galaxies, with morphological types ranging from Sa to Sm, including some barred galaxies. The LSB nature of their discs has been confirmed by a detailed photometric decomposition. With this aim, we derived the photometric parameters of the bulge and disc by applying a detailed decomposition of the surface brightness of the galaxy. We adopted the galaxy surface photometric 2D (GASP2D) code by Méndez-Abreu et al. (2008, see Figure 1). The structural parameters of the galaxies were derived assuming the galaxy surface-brightness distribution to be the sum of the contributions of a bulge, a disc and, if necessary, a bar. We fitted iteratively the model of the surface brightness to the pixels of the galaxy image using a nonlinear least squares minimisation.

The photometric and spectroscopic observations were carried out with the Very Large Telescope (VLT) during several runs between 2001 and 2008 with FORS2. For each galaxy the images were obtained with the R_special+76 filter and long-slit spectra on the major and minor axes were usually taken using the

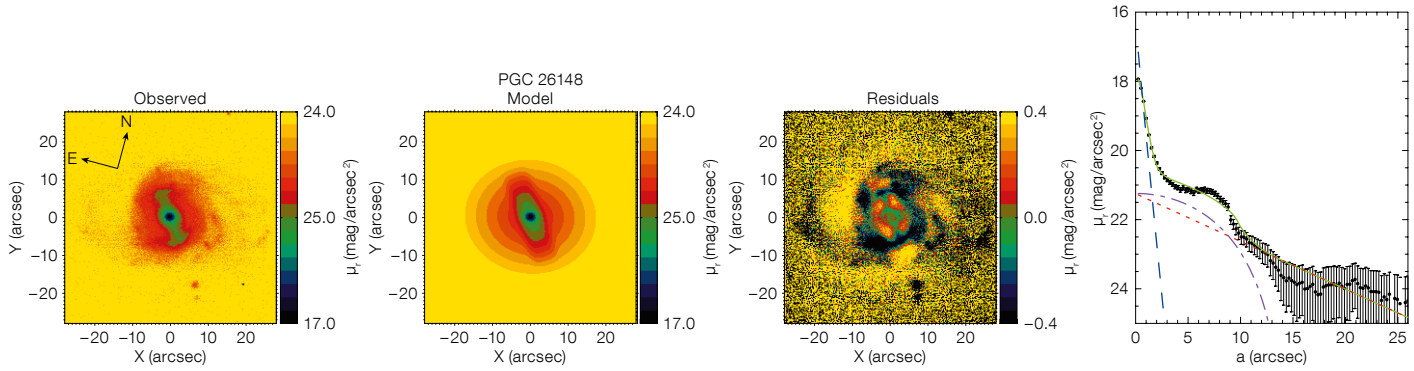

Figure 1. Two-dimensional photometric decomposition of PGC 26148. The FORS2 *r*-band image, best-fitting image, residual (i.e. observed-model) image and surface-brightness radial profile are shown (panels from left to right). The righthand panel shows the ellipse-averaged radial profile of the surface brightness measured from FORS2 (dotted line) and model image (green solid line). The dashed blue, dash-dotted purple, and dotted red lines represent the intrinsic surface-brightness radial profiles of the bulge, bar and disc, respectively.

grism GRIS_1400V+18 in combination with a 0.7-arcsecond slit that guarantees an instrumental velocity resolution of 33 km/s at 5000 Å.

The stellar kinematics were measured from the galaxy absorption features present in the wavelength range centred on the Hβ and Mg I lines by applying the gas and absorption line fitting (GANDALF; Sarzi et al., 2006) IDL package, adapted for dealing with the FORS2 spectra. The Mg, Fe and Hβ line-strength indices were measured from the flux-calibrated spectra of the eight sample galaxies following Morelli et al. (2004). We also measured the average iron index <Fe> = (Fe5270 + Fe5335)/2 and the combined magnesium–iron index [MgFe]' = $[Mg_b\ (0.72 \times Fe5270 + 0.28 \times Fe5335)]^{1/2}$ (Thomas et al., 2003). To account for the contamination of the Hβ line-strength index by the Hβ emission line, the Hβ index was measured from the galaxy spectrum after subtracting the contribution of the Hβ emission line.

Properties of the stellar populations in the central regions

The models of Thomas et al. (2003) predict the values of the line strength Lick indices for a single stellar population as a function of the age, metallicity and [α/Fe] ratio. The central values of the velocity dispersion, Mg_b, Mg_2, Hβ, <Fe>, and [MgFe]' were obtained by a weighted mean of all the measured data points within an aperture of radius 0.3 r_e for all the available spectra. From the central

Figure 2. Distribution of the central values of the Hβ and [MgFe]' indices (left panel) and the <Fe> and Mgb indices (right panel) measured over an aperture of 0.3 r_e for the sample galaxies. The lines indicate the models of Thomas et al. (2003). In the left panel, the age–metallicity grids are plotted with two different α/Fe enhancements: [α/Fe] = 0.0 dex (solid lines) and [α/Fe] = 0.5 dex (dashed lines). In the right panel, the [α/Fe] ratio–metallicity grids are plotted with two different ages: 2 Gyr (solid lines) and 6 Gyr (dashed lines). The green points are the values obtained for three LSB galaxies by Bergmann et al. (2003).

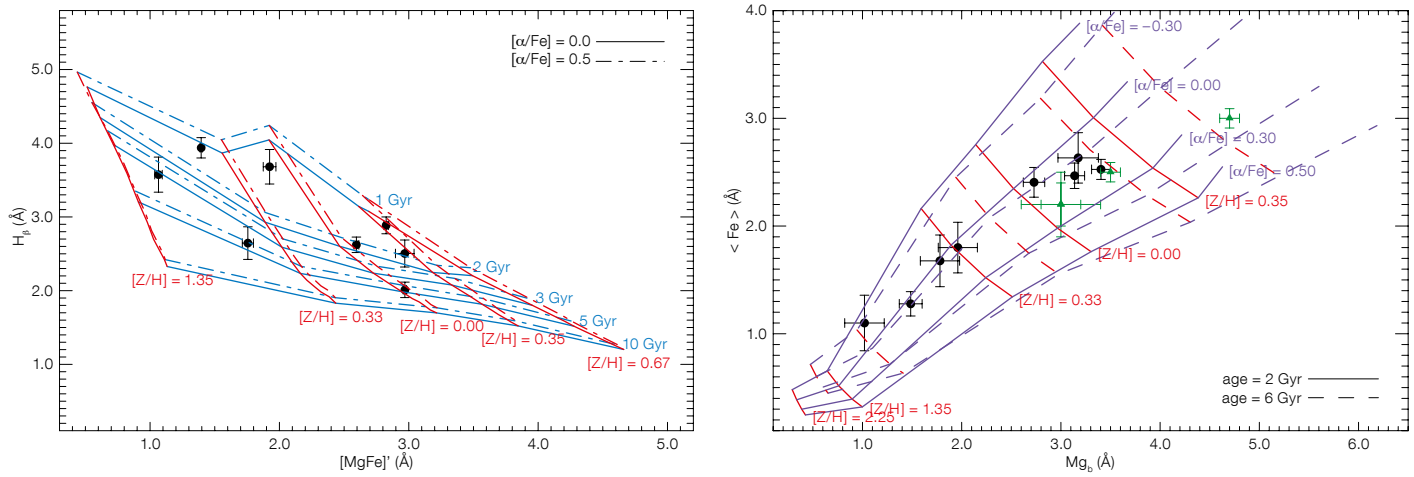

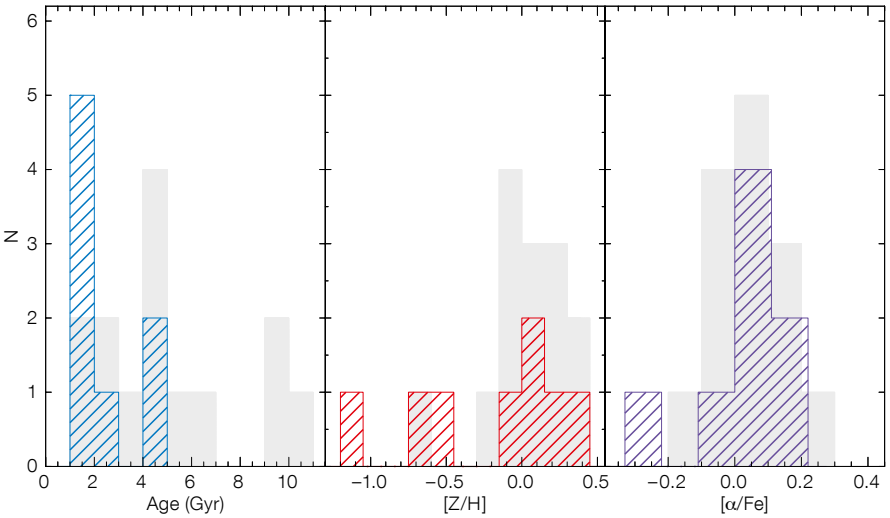

Figure 3. Distribution of the mean age (lefthand panel), total metallicity (central panel), and total α/Fe enhancement (righthand panel) for the stellar populations of the bulges of the sample galaxies. The distributions of the same quantities obtained by Morelli et al. (2008) for the bulges of HSB discs are plotted in grey for comparison.

values of the Lick indices we derived the mean age, total metallicity and total α/Fe enhancement of the stellar population in the central region of the bulge of the sample galaxies (see Figure 2).

The bulges are characterised by a very young stellar population, with a distribution of ages peaking at a value of 1.5 Gyr. They are characterised by ongoing star formation, confirming previous studies of a few LSB galaxies (Bergmann et al., 2003). The metallicity of the sample bulges spans a large range of values from high values ([Z/H] = 0.30 dex) to sub-solar metallicity ([Z/H] = –1.0 dex). Most display solar α/Fe enhancements. These properties closely resemble the properties of the bulges hosted in HSB galaxies (Figure 3) and they suggest a formation mechanism with a dissipative collapse with a short star formation timescale.

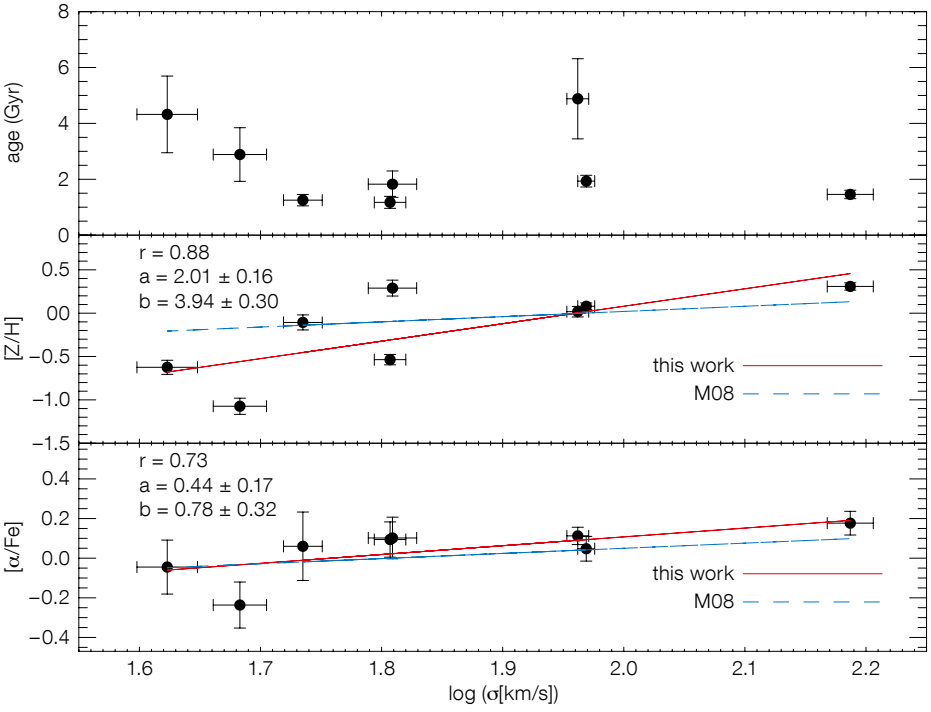

Figure 4. Mean age (upper panel), total metallicity (middle panel), and total α/Fe enhancement (lower panel) of the stellar populations of the bulges of the sample galaxies as a function of the central velocity dispersion. In each panel, the red solid and blue dashed lines represent the linear regression through the data points and the correlation found by Morelli et al. (2008) for the bulges of HSB galaxies, respectively. The Pearson correlation coefficient (*r*) and the coefficients of the linear fit are given.

For galaxies with sub-solar values of α/Fe enhancement, other mechanisms of bulge formation, such as the redistribution of disc material, because of the presence of a bar, or environmental effects need to be considered. The case of the bulge of ESO-LV 4880490 is particularly intriguing. The bulge of this barred galaxy has an intermediate age (3 Gyr), low metallicity, ([Z/H] = –1.07 dex) and sub-solar α/Fe ratio ([α/Fe] = –0.24 dex). These properties are consistent with a slow build-up within a scenario of secular evolution driven by the bar.

The correlation between the galaxy morphological type and the properties of the bulge stellar population is indicative of the possible interplay between the evolution of the bulge and disc. Thomas & Davies (2006) did not observe any correlation between the age and metallicity of the stellar population and galaxy morphology of the bulge, whereas Ganda et al. (2007) and Morelli et al. (2008) found a mild correlation, with early-type galaxies (S0–S0a) being older and more metal-rich than spiral galaxies (Sa–Sc). Because the above relationships are mostly driven by early-type galaxies, which are lacking in our sample, we do not observe any correlation between the galaxy morphological type (Sab–Sm) and the age, metallicity and α/Fe enhancement of our bulges. Nevertheless, we can exclude a strong interplay between the bulge and disc components.

In early-type galaxies and in the bulges of HSB galaxies the metallicity and α/Fe enhancement are well correlated with the central velocity dispersion. We find that

also for LSB galaxies the metallicity and α/Fe enhancement correlate with velocity dispersion (Figure 4) and this correlation is consistent with the results obtained in Morelli et al. (2008).

These relations are explained by chemo-dynamical models and cosmological hydrodynamic simulations of ellipticals and bulges as the result of a mass-dependent star formation efficiency. Low-mass galaxies have a lower efficiency in converting gas-phase metals into new stars, and this gives rise to a prolonged period of star formation and to lower α/Fe ratios. Our results suggest that this is also true for the bulges of LSB galaxies. We conclude that the most massive bulges of our sample galaxies are more metal-rich, and that they are characterised by shorter star formation timescales.

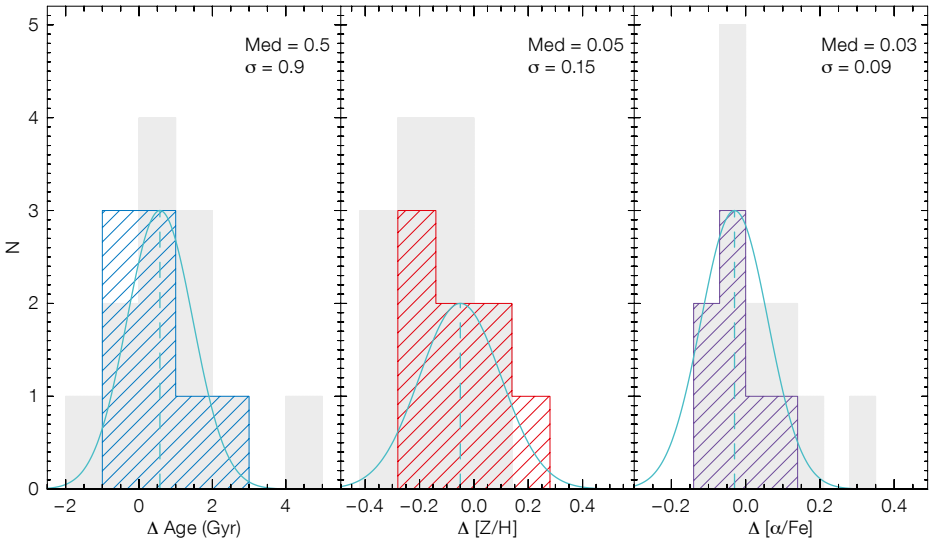

Figure 5. Distribution of the gradients of age (lefthand panel), metallicity (central panel), and α/Fe enhancement (righthand panel) for the sample bulges. The dashed line represents the median of the distribution and its value is reported. The solid line represents a Gaussian centred on the median value of the distribution, with σ reported. The distribution of the same quantities obtained by Morelli et al. (2008) for the bulges of HSB discs is shown in grey for comparison.

Properties of the stellar populations in the bulge region

The contamination of the bulge light by the contribution coming from the underlying disc stellar component is a well-known problem that deserves particular care. To reduce the impact of this effect in the derived stellar population properties as much as possible, we evaluated the gradient inside r_{bd}, the radius where the bulge and disc give the same contribution to the total surface brightness (Morelli et al., 2008). This did not completely remove the contaminations, but it always ensured a similar degree of contamination when comparing the gradients of different galaxies. For each galaxy, we have derived the Mg_2, Hβ, and <Fe> line-strength indices at the radius r_{bd}.

The corresponding ages, metallicities and α/Fe enhancements were derived by using the stellar population models of Thomas et al. (2003), as for the central values. The gradients of the properties of the bulge stellar population were derived from the values of age, metallicity and α/Fe enhancement in the radial range out to r_{bd}. All the sample bulges show no age gradient within the error bars, except for ESO-LV 2060140 and PGC 26148, which are characterised by a shallow gradient. In spite of the peak at Δ([Z/H]) = –0.15, the median of the number distribution of the metallicity gradients is consistent with Δ([Z/H]) = 0 (see Figure 5, middle panel). Also, the number distribution of the gradients of α/Fe enhancements has a median Δ[α/Fe] = 0 (Figure 5, righthand panel). In all the observed distributions, most of the deviations from the median values can be explained as a result only of the errors in the estimates of the gradients. The absence of significant age and α/Fe gradients is in agreement with the earlier findings for early-type galaxies and bulges of unbarred and barred HSB galaxies. However, negative gradients of metallicity are observed in the radial profiles of many early-type galaxies and in the bulges of HSB galaxies.

In the models, the presence of a negative metallicity gradient predicts a formation scenario of the bulges in LSB galaxies via dissipative collapse, when a strong interplay between the star formation timescale and gas flows is taken into account in order to explain the absence of any α/Fe gradient (Pipino et al., 2008). However, pure dissipative collapse cannot explain the formation of all the sample bulges; other phenomena, such as mergers or acquisition events, need to be invoked to account for the formation of those bulges that do not show any metallicity gradient. The metallicity gradients are plotted as a function of the metallicity in the galaxy centre in the lefthand panel of Figure 6. Only the bulges of LSB galaxies with higher metallicity (–0.1 < [Z/H] < 0.4) are consistent with the correlation found by Morelli et al. (2008) for the bulges in HSB galaxies and early-type galaxies, respectively. This is not the case for the few remaining bulges with a very low central metallicity value (–1.1 < [Z/H] < –0.5). If confirmed with more firm statistics, such a result would favour the importance of dissipative collapse in the assembly of bulges (Arimoto & Yoshii, 1987).

No correlation has been found between the central value and gradient of α/Fe enhancement (see the righthand panel of Figure 6). This is in agreement with earlier findings for early-type galaxies and spiral galaxies, and it is expected because of the absence of gradients in the α/Fe radial profiles of the sample galaxies.

The common nature of bulges in LSB and HSB galaxies

We have highlighted the fact that bulges hosted by LSB galaxies share many structural and chemical properties with the bulges of HSB galaxies. Such a similarity suggests that they possibly had common formation scenarios and evolu-

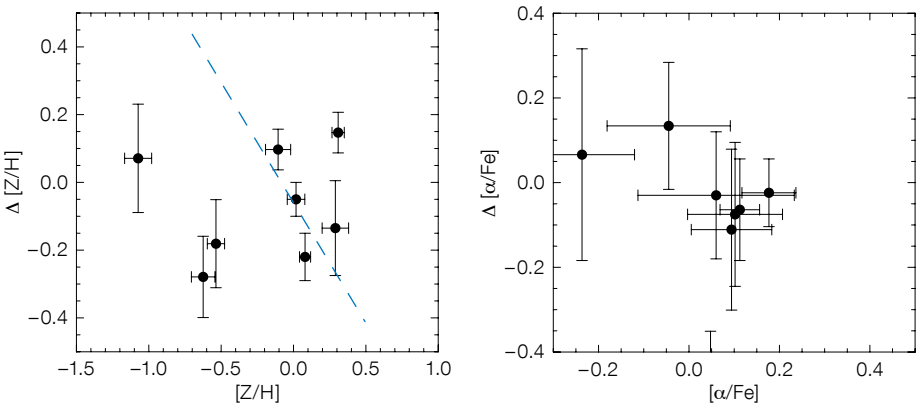

Figure 6. Gradient and central value of metallicity (lefthand panel) and α/Fe enhancement (righthand panel) for the sample bulges. In the lefthand panel, the dashed blue line represents the linear regression obtained for the bulges of HSB galaxies by Morelli et al. (2008).

tion histories. Our findings are in agreement with, and also extend, the previous results inferred by McGaugh, Schombert & Bothun (1995) and Beijersbergen et al. (1999), who compared the photometric properties of the bulges of LSB and HSB galaxies, and by Coccato et al. (2008), who performed a detailed analysis of the kinematical and mass distribution properties of the bulge of the LSB galaxy ESO 323-G064. The fact that bulges hosted in galaxies with very different discs are remarkably similar, rules out significant interplay between the bulge and disc components and provides further support for earlier findings (Thomas & Davies, 2006; Morelli et al., 2008). In order to provide a definite confirmation, this prediction requires a detailed comparison between the properties of the stellar populations of both bulges and discs in LSB galaxies.

References

Annibali, F. et al. 2007, A&A, 463, 455
Arimoto, N. & Yoshii, Y. 1987, A&A, 173, 23
Beijersbergen, M., de Blok, W. J. G. & van der Hulst, J. M. 1999, A&A, 351, 903
Bekki, K. & Shioya, Y. 1999, ApJ, 513, 108
Bergmann, M. P., Jørgensen, I. & Hill, G. J. 2003, AJ, 125, 116
Bothun, G., Impey, C. & McGaugh, S. 1997, PASP, 109, 745
Coccato, L. et al. 2008, A&A, 490, 589
Galaz, G. et al. 2006, AJ, 131, 2035
Ganda, K. et al. 2007, MNRAS, 380, 506
Hopkins, P. F. et al. 2009, ApJS, 181, 135
McGaugh, S. S. et al. 1995, AJ, 109, 2019
Méndez-Abreu, J. et al. 2008, A&A, 478, 353
Moorthy, B. K. & Holtzman, J. A. 2006, MNRAS, 371, 583
Morelli, L. et al. 2004, MNRAS, 354, 753
Morelli, L. et al. 2008, MNRAS, 389, 341
Morelli, L. et al. 2012, MNRAS, 423, 962
Pipino, A., D'Ercole, A. & Matteucci, F. 2008, A&A, 484, 679
Sánchez-Blázquez, P. et al. 2006, A&A, 457, 809
Sarzi, M. et al. 2006, MNRAS, 366, 1151
Thomas, D., Maraston, C. & Bender, R. 2003, MNRAS, 339, 897
Thomas, D. & Davies, R. L. 2006, MNRAS, 366, 510

ESO and Joe DePasquale

MPG/ESO 2.2-metre telescope and Wide Field Imager colour picture of the isolated spiral galaxy NGC 3621. Broadband (*B* and *V*) and narrowband emission line ([O III] and H-alpha) images were combined and highlight the H II regions and young stars in the spiral arms. NGC 3621 appears to have no bulge and yet its centre harbours an active nucleus; the distance, determined from photometry of Cepheid variable stars, is about 6.2 Mpc. More information can be found in Release 1104.